

Synthesis and catalytic activity of μ -oxo ruthenium(IV) porphyrin species to promote amination reactions

Paolo Zardi^a, Daniela Intrieri^b, Daniela Maria Carminati^b, Francesco Ferretti^b,
Piero Macchi^c and Emma Gallo^{*b}[‡]

^aDepartment of Chemical Sciences of Padua University, Via F. Marzolo, 1-35131 Padua, Italy

^bChemistry Department of Milan University, Via C. Golgi 19, 20133 Milan, Italy

^cDepartment of Chemistry and Biochemistry of University of Berne, Freiestrasse 3, CH-3012 Berne, Switzerland

Dedicated to Professor Tomás Torres on the occasion of his 65th birthday

Received 29 January 2016

Accepted 18 March 2016

ABSTRACT: This work describes the synthesis of ruthenium(IV) μ -oxo porphyrin complexes of general formula $[\text{Ru}^{\text{IV}}(\text{TPP})(\text{X})]_2\text{O}$ which have been applied as catalysts in nitrene transfer reactions using aryl azides (ArN_3) as nitrene sources. Collected data indicated that the catalytic efficiency of $[\text{Ru}^{\text{IV}}(\text{TPP})(\text{OCH}_3)]_2\text{O}$ was comparable to that of $\text{Ru}^{\text{II}}(\text{TPP})\text{CO}$ because of their analogous reactivity towards aryl azides to give the same catalytically active *bis*-imido species $\text{Ru}^{\text{VI}}(\text{TPP})(\text{ArN})_2$. The reaction of $[\text{Ru}^{\text{IV}}(\text{TPP})(\text{OCH}_3)]_2\text{O}$ with Ph_3CN_3 or $(\text{CH}_3)_3\text{SiN}_3$ afforded $[\text{Ru}^{\text{IV}}(\text{TPP})(\text{N}_3)]_2\text{O}$ which was fully characterised, its molecular structure was also determined by single crystal X-ray analysis.

KEYWORDS: homogeneous catalysis, ruthenium, amination, azide.

INTRODUCTION

The development of efficient synthetic procedures to attain aminated compounds is of paramount importance due to pharmaceutical and/or biologic behaviors of aza-containing molecules [1]. Amongst all the catalysts capable of promoting amination reactions, ruthenium(II) porphyrin complexes [2–4] show a good efficiency in catalysing the amination of saturated and unsaturated hydrocarbons by using different classes of aminating agents such as aryl iminoiodinanes ($\text{RN}=\text{IAr}$) [5], amines in the presence of oxidant species [6] and organic azides (RN_3) [7–11]. Numerous structural modifications of the porphyrin skeleton were carried out to improve the catalytic performance which can also be modulated by the electronic nature of the axial ligands onto the ruthenium(II) center [12, 13]. Based on the fact that the catalytic activity can be fine-tuned by the metal oxidation state, ruthenium(IV) [14, 15] and ruthenium(VI) [10, 16,

17] porphyrin catalysts were tested and their catalytic efficiency were compared to that of ruthenium(II) porphyrin complexes. Recorded data showed that high-valent ruthenium species are competent amination catalysts which strongly reinforce the hypothesis of their formation during ruthenium(II)-catalysed reactions, as suggested by several theoretical investigations [18–20].

Concerning the use of ruthenium(IV) porphyrin catalysts, C. M. Che and co-authors reported very good results on the activity of differently substituted $\text{Ru}^{\text{IV}}(\text{porphyrin})\text{Cl}_2$ [14, 15] complexes to promote C–H bond nitrene insertions but, to the best of our knowledge, the catalytic activity of dimeric ruthenium(IV) porphyrin species to promote amination reactions have not yet been reported. The synthesis of oxo-bridged dimers was studied in the early 80's [21] and is favored by using ruthenium(II)-carbonyl complexes of unhindered porphyrin ligands [22, 23], such as TPP (TPP = dianion of tetraphenylporphyrin) and OEP (OEP = dianion of octaethylporphyrin) as starting materials. The first report concerns the oxidation of $\text{Ru}^{\text{II}}(\text{OEP})\text{CO}$ by *tert*-butylhydroperoxide to yield the μ -oxo complex $[\text{Ru}^{\text{IV}}(\text{OEP})(\text{OH})]_2\text{O}$ [24], which showed

[‡]SPP full member in good standing

*Correspondence to: Emma Gallo, email: emma.gallo@unimi.it

an unexpected stability. In fact μ -oxo dimers can easily exchange the axial ligand under acidic conditions achieving compounds of the general formula $[\text{Ru}^{\text{IV}}(\text{porphyrin})(\text{L})_2\text{O}]$ [21]. The catalytic employment of μ -oxo ruthenium porphyrins is scarce and only recently R. Zhang and co-workers [25, 26] reported on the use of these dimeric species in promoting the oxidation of hydrocarbons upon photochemical activation.

Hence, we focused our attention on the synthesis of μ -oxo ruthenium porphyrin complexes to investigate their reactivity with organic azides and their catalytic activity in amination reactions.

RESULTS AND DISCUSSION

We started studying the reaction of $[\text{Ru}^{\text{II}}(\text{TPP})(\text{CO})(\text{MeOH})]$ (**1**) with *m*CPBA (*meta*-chloroperbenzoic acid) which formed $[\text{Ru}^{\text{IV}}(\text{TPP})(\text{mCB})_2\text{O}]$ complex (**2**) where two *meta*-chlorobenzoate (*m*CB) anions were present on the ruthenium axial positions. Complex **2** was unequivocally identified by MS and NMR spectroscopy which showed strongly shifted signals for the aromatic protons of *m*CB moieties. We also observed the typical signal pattern of a μ -oxo tetraphenylporphyrin complex, where the aromatic protons of the *meso*-phenyl groups were split into five different signals (Fig. 1). Complex **2** was obtained in a 39% yield and the missing mass balance was due to the partial decomposition of **2** into $[\text{Ru}^{\text{IV}}(\text{TPP})(\text{OCH}_3)_2\text{O}]$ (**3**) during the chromatographic purification with $\text{CH}_2\text{Cl}_2/\text{MeOH}$. Complex **3** was obtained

in a 40% yield and recorded analytical data were in accord to those reported in literature [21].

We synthesised complex **3** in high yields (81% yield) by reacting complex **1** with a slight excess of the oxidant *m*CPBA (8,0 eq.) in a $\text{MeOH}/\text{CH}_2\text{Cl}_2$ mixture in the convenient ratio of 10:1, which limited the formation of complex **2** and assured the complete conversion of the starting complex **1**.

Complexes **2** and **3** were both tested as catalysts of the cumene amination and only complex **3** promoted the synthesis of the corresponding benzylic amine in 65% yield (entry 1, Table 1). Thus, complex **3** was tested as the catalyst for the nitrene transfer reactions shown in Scheme 1 by using aryl azides as nitrogen sources and obtained aza-derivatives are reported in Table 1.

As shown in Table 1, compound **3** was active in promoting benzylic (entries 1–7) and allylic (entry 8) aminations as well as aziridination reactions (entry 9). In order to evaluate the catalytic efficiency of **3** for the benzylic amination, the amination of cumene was run in the presence of the low catalyst loading of 0.025% mol to obtain **4** in 65% yield. Complex **3** was also active in promoting the amination of less reactive benzylic substrates such as methyl phenylacetate (entry 6) and methyl dihydrocinnamate (entry 7), which were transformed into corresponding amino esters **9** and **10**. Concerning the allylic amination of cyclohexene (entry 8) the reaction efficiency was independent from the electronic feature of the starting azide and similar yields were achieved in the synthesis of compounds **11** and **12**. The low yield obtained in the synthesis of compound **13** can be due to a

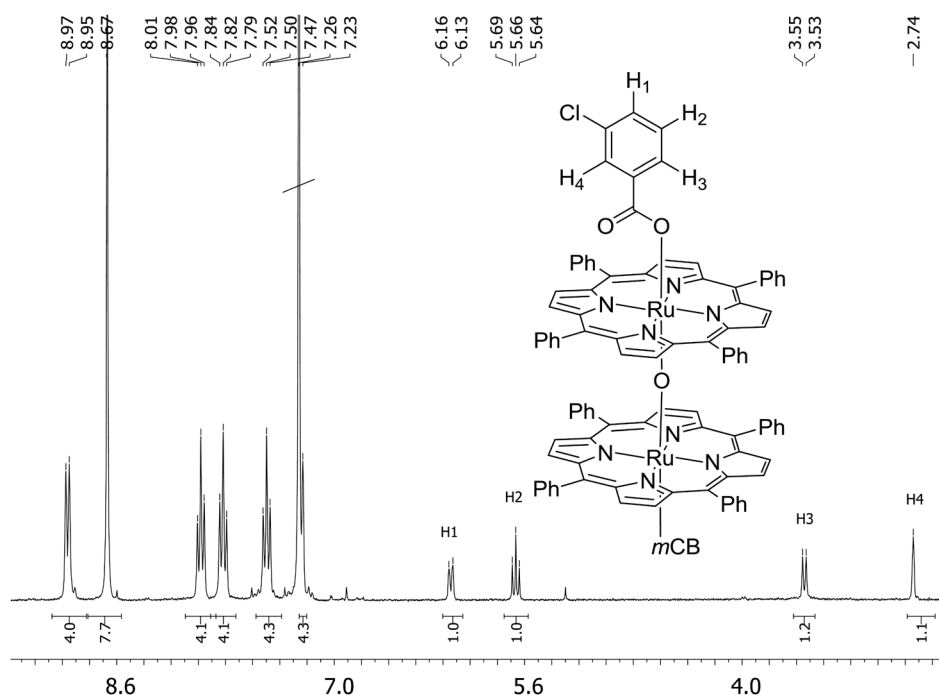
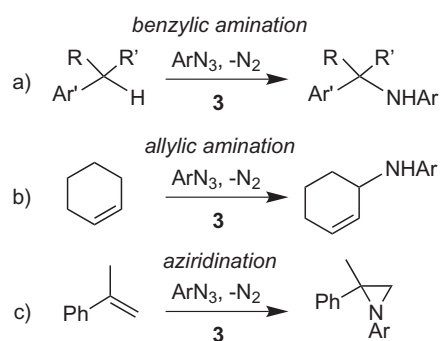


Fig. 1. Structure and ^1H NMR spectrum of $[\text{Ru}^{\text{IV}}(\text{TPP})(\text{mCB})_2\text{O}]$ complex (**2**)



Scheme 1. Nitrene transfer reactions catalysed by complex **3**

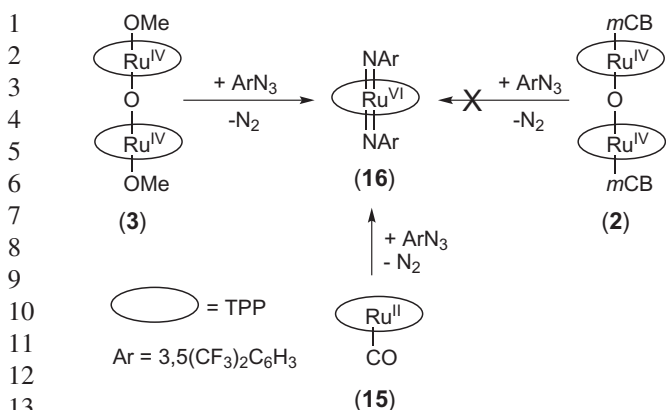
partial inhibition of the catalytic activity by the coordination of the substrate methoxy group to the ruthenium center. As reported in entry 9 of Table 1, complex **3** was also a very good catalyst for the aziridination of α -methylstyrene which afforded the desired aziridine **14** in a very short reaction time and a quantitative yield. Even if **3** demonstrated to be a competent and versatile amination catalyst, collected catalytic data are comparable to those already achieved by using Ru(TPP)CO (**15**) as the catalytic species [10, 11, 18, 27].

In view of the observed similarity between the catalytic behavior of complexes [Ru^{IV}(TPP)(OCH₃)₂O] (**3**) and Ru^{II}(TPP)(CO) (**15**), we reacted μ -oxo derivatives **2** and

Table 1. Synthesis of aza-derivatives **4–14** catalysed by [Ru^{IV}(TPP)(OCH₃)₂O] (**3**)^a

Entry	Reagent	Product	Ar	T, h ^b	Yield, % ^c
1			3,5(CF ₃) ₂ C ₆ H ₃ , 4	0.5	65
2			3,5(CF ₃) ₂ C ₆ H ₃ , 5	1.5	55
3			3,5(CF ₃) ₂ C ₆ H ₃ , 6	5.5	80
4			3,5(CF ₃) ₂ C ₆ H ₃ , 7	2	65
5			3,5(CF ₃) ₂ C ₆ H ₃ , 8	1.5	90
6 ^d			3,5(CF ₃) ₂ C ₆ H ₃ , 9	6	44
7 ^d			3,5(CF ₃) ₂ C ₆ H ₃ , 10	5	70
			3,5(CF ₃) ₂ C ₆ H ₃ , 11	0.75	65
8 ^e			4(^t Bu)C ₆ H ₄ , 12	3	60
			4(OCH ₃)C ₆ H ₄ , 13	1.5	20
9 ^f			3,5(CF ₃) ₂ C ₆ H ₃ , 14	0.1	99

^aCatalyst **3** (2.6×10^{-5} mol, 1.0% with respect to ArN₃) in 25.0 mL of refluxing substrate. ^bTime required for the complete azide conversion monitored by IR spectroscopy. ^cDetermined by ¹H NMR spectroscopy (2,4-dinitrotoluene as the internal standard). ^dCatalytic ratio **3** (2.6×10^{-4} mol)/azide/substrate = 1:10:250 in 25.0 mL of refluxing benzene. ^eCatalytic ratio **3** (5.2×10^{-5} mol)/azide/substrate = 1:50:250 in 25.0 mL of refluxing benzene. ^fCatalytic ratio **3** (2.6×10^{-5} mol)/azide/substrate = 1:100:250 in 25.0 mL of refluxing benzene.



Scheme 2. Stoichiometric reaction of complexes **2** and **3** with 3,5-*bis*(trifluoromethyl)phenyl azide

3 with a slight excess of 3,5-*bis*(trifluoromethyl)phenyl azide (Ru/azide = 1:3) in order to discover the nature of catalytic intermediates and to investigate whether similar or different mechanistic pathways are involved when ruthenium(IV) catalysts are used instead of ruthenium(II) complexes.

Complex **2** did not react with 3,5-*bis*(trifluoromethyl)phenyl azide even under light irradiation, whilst **3** was converted into the *bis*-imido $\text{Ru}^{\text{VI}}(\text{TPP})(3,5\text{-}(\text{CF}_3)_2\text{C}_6\text{H}_3\text{N}_2)$ (**16**) after 4 h (Scheme 2). As already reported [10, 17], complex **16** can be also obtained from the stoichiometric reaction of complex $\text{Ru}(\text{TPP})\text{CO}$ (**15**) with 3,5-*bis*(trifluoromethyl)phenyl azide.

These results suggested that the formation of *bis*-imido ruthenium(VI) active species was independent from the oxidation state of the starting ruthenium complex which can be considered a pre-catalyst of the amination reaction. Achieved data also explain the catalytic inactivity shown by complex **2** in the amination of cumene, it did not react with the involved azide and consequently it was not converted into the catalytically active ruthenium(VI) intermediate.

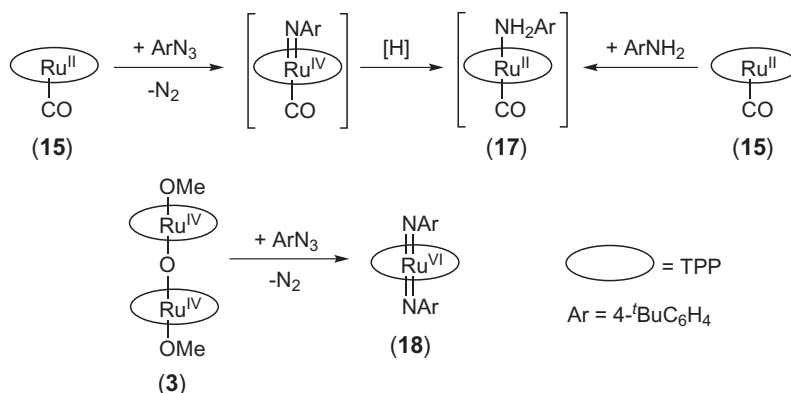
Given the reactivity of complex **3** towards azides, it was investigated for the synthesis of *bis*-imido

complexes which cannot be obtained by directly reacting ruthenium(II) porphyrin derivatives with aryl azides. As already reported [10, 17], this synthetic strategy was effective by using electron poor aryl azides as the starting material whereas *bis*-imido complexes were not obtained when electron rich aryl azides were employed. This can be due to the reaction of the initially formed *mono*-imido $\text{Ru}^{\text{IV}}(\text{porphyrin})(\text{ArN})\text{CO}$ with traces of water to yield $\text{Ru}^{\text{II}}(\text{porphyrin})(\text{ArNH}_2)\text{CO}$. This decomposition pathway was previously observed in the reaction between $\text{Ru}^{\text{II}}(\text{TPP})\text{CO}$ and 4-*tert*-butylphenyl azide (4- $\text{BuC}_6\text{H}_4\text{N}_3$) which formed $\text{Ru}^{\text{II}}(\text{TPP})(4\text{-BuC}_6\text{H}_4\text{NH}_2)\text{CO}$ (**17**) in good yields (Scheme 3) [10]. Analytical data of **17** were in accord with those of the compound synthesised by directly reacting $\text{Ru}(\text{TPP})\text{CO}$ (**15**) with 4- $\text{BuC}_6\text{H}_4\text{NH}_2$.

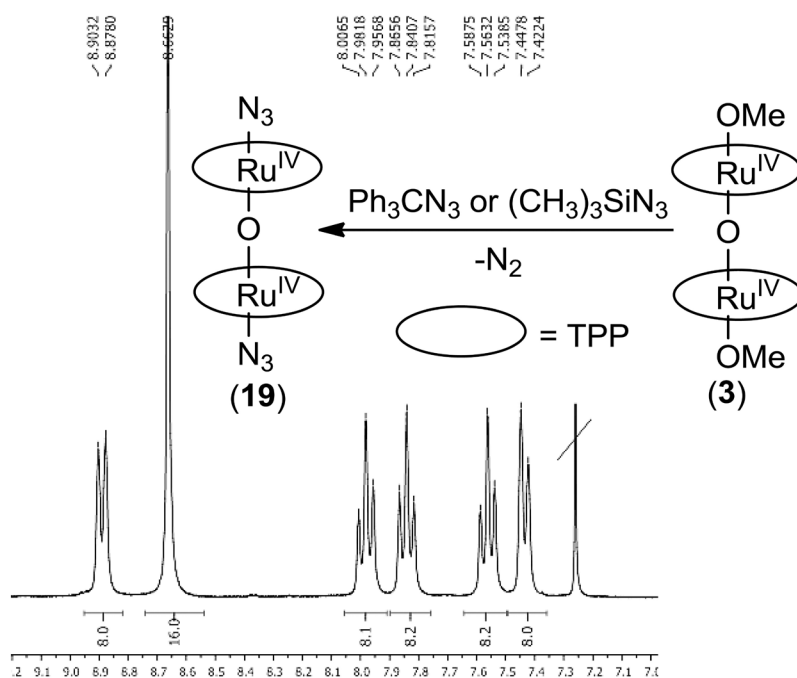
The replacement of $\text{Ru}^{\text{II}}(\text{TPP})\text{CO}$ (**15**) by $[\text{Ru}^{\text{IV}}(\text{TPP})(\text{OCH}_3)_2\text{O}]$ (**3**) in the reaction with 4- $\text{BuC}_6\text{H}_4\text{N}_3$ afforded complex $\text{Ru}^{\text{VI}}(\text{TPP})(4\text{-BuC}_6\text{H}_4\text{N}_2)$ (**18**) to suggest an important effect of the metal oxidation state of the starting ruthenium complexes in the reaction with aryl azides.

It can be suggested that the reaction between **3** and 4- $\text{BuC}_6\text{H}_4\text{N}_3$ followed a different pathway during which the unstable ruthenium(IV) *mono*-imido complex was not formed and consequently the decomposition process leading to **17** was avoided. Complex **18** was fully characterised and its reactivity was tested in both stoichiometric nitrene transfer and catalytic reactions by using cyclohexene as the substrate. In both cases complex **18** was completely inactive to indicate that the reactivity of nitrene functionalities is strongly related to the electron density on ruthenium-imido functionality which in turn depends on the electronic nature of substituents onto the “ArN” moiety as proposed by a previous theoretical study [19].

In order to expand the reaction scope, complex **3** was reacted with a stoichiometric amount of tosyl azide, adamantyl azide and benzyl azide. In the first two cases no reaction occurred, whilst in the last case the reaction achieved unidentified products. When complex **3** was reacted with organic azides (RN_3) displaying a good *R* leaving group for electrophilic substitutions



Scheme 3. Synthesis of complexes **17** and **18**



Scheme 4. Synthesis and ^1H NMR spectrum of complex 19

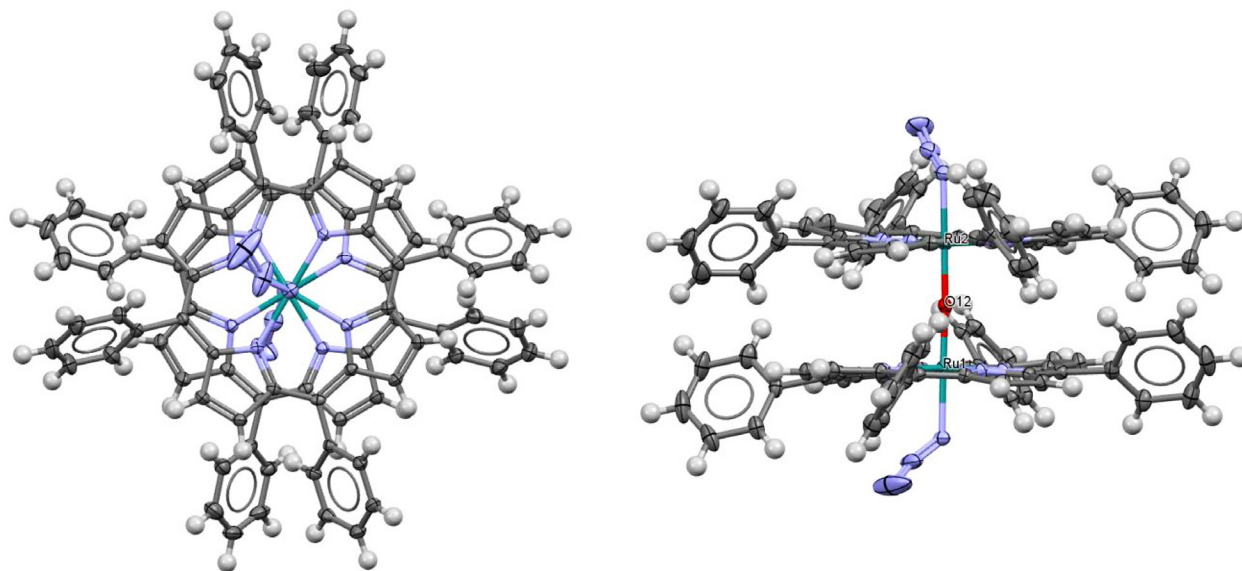


Fig. 2. Top and side view of the molecular structure of **19**. Atomic displacement parameters are shown as ellipsoids at 50% probability level. Ru atoms are in green, O atom is in red, N atoms are in blue, C atoms are in dark grey and H atoms in light grey. For sake of clarity, the disorder of azido group has been removed and only the dominant orientation of each group is shown

(R = trityl or trimethylsilyl) a new μ -oxo dimer complex $[\text{Ru}^{\text{IV}}(\text{TPP})(\text{N}_3)]_2\text{O}$ (**19**) was obtained at room temperature (Scheme 4).

Compound **19** was completely characterised and a slow diffusion of a CHCl_3 solution of $[\text{Ru}(\text{TPP})(\text{N}_3)]_2\text{O}$ into n -hexane gave crystals suitable for the molecular structure determination by X-ray diffraction analysis (Fig. 2, Table 2).

The crystal has a monoclinic $\text{P}2_1/n$ space group, with one independent molecule in the asymmetric unit and therefore four molecules in the unit cell. At least one molecule of the crystallization solvent is localised (although refined with a disordered model). A rather large void volume (780 \AA^3 per unit cell) indicates that very likely other solvent molecules (3 per asymmetric unit) may be present, but their disorder is so strong that they

Table 2. Crystal data and structure refinement for **19**

Empirical formula	$C_{88}H_{56}N_{14}ORu_2 \cdot CHCl_3$	
Formula weight	1646.96	
Temperature	173(2) K	
Wavelength	0.71069 Å	
Crystal system	Monoclinic	
Space group	P 2 ₁ /n	
Unit cell dimensions	$a = 13.89880 (10) \text{ \AA}$	$\alpha = 90^\circ$.
	$b = 31.9489 (3) \text{ \AA}$	$\beta = 107.5230 (10)^\circ$.
	$c = 18.4576 (2) \text{ \AA}$	$\gamma = 90^\circ$.
Volume	7815.79 (13) Å ³	
Z	4	
Density (calculated)	1.399 Mg/m ³	
Absorption coefficient	0.547 mm ⁻¹	
F(000)	3340	
Crystal size	0.3 × 0.2 × 0.1 mm ³	
Theta range for data collection	1.621 to 25.347°.	
Index ranges	-16 ≤ h ≤ 16, -38 ≤ k ≤ 38, -22 ≤ l ≤ 22	
Reflections collected	58274	
Independent reflections	14312 [R(int) = 0.0336]	
Completeness to theta = 25.000°	100.0%	
Refinement method	Full-matrix least-squares on F ²	
Data/restraints/parameters	14312/72/1031	
Goodness-of-fit on F ²	1.041	
Final R indices [I > 2σ(I)]	R ₁ = 0.0663, wR ₂ = 0.1932	
R indices (all data)	R ₁ = 0.0754, wR ₂ = 0.2030	
Largest diff. peak and hole	5.011 and -1.593 e.Å ⁻³	

cannot be easily localised even analysing the residual electron density. The molecular structure of **19** (see Fig. 2) is dominated by the sandwich-like aggregation of the two porphyrins that trap the O atoms exactly in the middle between the two Ru atoms (1.796(3) and 1.798(3) Å for O12-Ru1 and O12-Ru2, respectively). The two average planes are almost exactly parallel to each other, although the porphyrin skeletons are not exactly flat. Moreover, the phenyl substituents clearly produce large steric hindrance and they have a conformation tilted by 50–65° with respect to the porphyrin planes. Repulsions between atoms of the two porphyrin skeletons and repulsion between the phenyl rings of the two porphyrins, induce a staggered-like conformation by making the two porphyrins rotated by *ca.* 28° with respect to the Ru–Ru axis. This feature is rather common in M–M bonded di-porphyrin complexes with the only exception of (TPP)Mo–Re(OEP), featuring a quadruple M–M bond [28], which is perfectly eclipsed. For systems like **19**, with a bridging atom making the

porphyrin–porphyrin distance larger, the staggered conformation is still the most common, although many eclipsed structures are also known. On each Ru atom, *trans* to the bridging O, an azide group is coordinated. The potential around this ligand is rather flat, producing a large dynamic disorder that could not be eliminated even with a data collection at low temperature. Each azide has at least two orientations (only the major component is shown in Fig. 2), anyway the coordination to Ru features the classical bent mode: Ru–N–N angles are 126.7(4) and 121.2(10)° for the main orientations of azide at Ru(1) and Ru(2), respectively. This is in keeping with the average values known for Ru–azido complexes. The Ru–N bonds are instead somewhat shorter than the average values from the literature for Ru^{IV}–N₃ bonds (2.05 vs. 2.13 Å), which could reflect the large atomic motion. The N–N distances of the azides are even more affected by the orientational disorder and the large thermal motion, therefore their accuracy is lower and does not allow

precise comparisons with other structures. The bonds of the porphyrin skeleton to Ru atoms are perfectly matching the standard values (2.05 Å).

EXPERIMENTAL

General

Unless otherwise specified, all the reactions were carried out in a nitrogen atmosphere employing standard Schlenk techniques and magnetic stirring. Toluene, *n*-hexane and benzene were dried by M. Braun SPS-800 solvent purification system. THF, α -methylstyrene, cyclohexene, cumene and decalin over sodium and stored under nitrogen. 1,2-Dichloroethane and CH_2Cl_2 were distilled over CaH_2 and immediately used. Commercial *m*CPBA (77%) was purified using a reported procedure [29] and stored at -20°C . Aryl azides [27, 30], $[\text{Ru}^{\text{II}}(\text{TPP})(\text{CO})(\text{CH}_3\text{OH})]$ (**1**) [31], $[\text{Ru}^{\text{IV}}(\text{TPP})(\text{OCH}_3)_2]\text{O}$ (**3**) [21], $\text{Ru}^{\text{II}}(\text{TPP})\text{CO}$ (**15**) [22] and $\text{Ru}^{\text{VI}}(\text{TPP})(3,5\text{-}(\text{CF}_3)_2\text{C}_6\text{H}_3\text{N})_2$ (**16**) [17] were synthesised by methods reported in the literature or using minor modifications. The purity of hydrocarbons and aryl azides employed was checked by GC-MS or ^1H NMR analysis. All the other starting materials were commercial products used as received. NMR spectra were recorded at room temperature, unless otherwise specified, on a Bruker avance 300-DRX, operating at 300 MHz for ^1H , at 75 MHz for ^{13}C and at 282 MHz for ^{19}F . Chemical shifts (ppm) are reported relative to TMS. The ^1H NMR signals of the compounds described in the following have been attributed by COSY and NOESY techniques. Assignments of the resonances in ^{13}C NMR were made using the APT pulse sequence and HSQC and HMBC techniques. GC-MS analyses were performed on a Shimadzu QP5050A equipped with Supelco SLB -5 ms capillary column (L 30 m \times I.D. 0.25 mm \times 0.25 μm film thickness). GC analyses were performed on a Shimadzu GC -2010 equipped with a Supelco SLB -5ms capillary column (L 10 m \times I.D. 0.1 mm \times 0.1 μm film thickness). Infrared spectra were recorded on a Varian Scimitar FTS 1000 spectrophotometer. UV-vis spectra were recorded on an Agilent 8453E instrument. Elemental analyses and mass spectra were recorded in the analytical laboratories of Milan University. The collected analytical data for *N*-(2-phenylpropan-2-yl)-3,5-bis(trifluoromethyl)aniline (**4**) [11]; *N*-phenyl-3,5-bis(trifluoromethyl)aniline (**5**) [11]; *N*-(1-phenylethyl)-3,5-bis(trifluoromethyl)aniline (**6**) [32]; *N*-(2-methyl-1-phenylpropyl)-3,5-bis(trifluoromethyl)aniline (**7**) [17]; *N*-(3,5-bis(trifluoromethyl)phenyl)-2,3-dihydro-1*H*-inden-1-amine (**8**) [11]; methyl 2-((3,5-bis(trifluoromethyl)phenyl)amino)-2-phenylacetate (**9**) [33]; methyl 3-((3,5-bis(trifluoromethyl)phenyl)amino)-3-phenylpropanoate (**10**) [33]; *N*-(cyclohex-2-en-1-yl)-3,5-bis

(trifluoromethyl)aniline (**11**) [10]; 4-(*tert*-butyl)-*N*-(cyclohex-2-en-1-yl)aniline (**12**) [10]; *N*-(cyclohex-2-en-1-yl)-4-methoxyaniline (**13**) [10]; 2-methyl-1-(4-nitrophenyl)-2-phenylaziridine (**14**) [34] were in agreement with those reported in literature.

Synthesis

Synthesis of $[\text{Ru}^{\text{IV}}(\text{TPP})(m\text{CB})_2]\text{O}$ (2**).** Complex **1** (102 mg, 1.32×10^{-4} mol) was suspended in CH_2Cl_2 (20 mL) and a solution of *m*CPBA (123 mg, 7.13×10^{-4} mol) in CH_2Cl_2 (25 mL) was added dropwise in 30 min and in air. The initial red suspension turned into a dark red solution. The reaction was stirred for 1.5 h and the TLC analysis (Al_2O_3 , CH_2Cl_2) revealed the presence of unreacted complex **1**. An additional amount of *m*CPBA (52 mg, 3.0×10^{-4} mol) was added and the solution was stirred for 3 h. TLC and IR analyses (nujol, $\nu_{\text{C=O}}$ of **1** at 1939 cm^{-1}) showed the complete consumption of starting **1**. The solution was concentrated to about 20 mL and filtered through a short (5 cm) alumina column. The product fraction was evaporated to dryness and the resulting dark solid was dried *in vacuo* (47 mg, 39%). ^1H NMR (300 MHz, CDCl_3): δ , ppm 8.96 (8H, d, $J = 7.6$ Hz, H_α), 8.67 (16H, s, H_β), 7.98 (8H, t, $J = 7.2$ Hz, H_m), 7.82 (8H, t, $J = 7.5$ Hz, H_p), 7.50 (8H, t, $J = 7.6$ Hz, H_m), 7.25 (8H, overlaps with chloroform signal, H_α), 6.14 (2H, d, $J = 7.9$ Hz, H_3), 5.66 (2H, t, $J = 7.8$ Hz, H_3), 3.54 (2H, d, $J = 7.8$ Hz, H_1), 2.74 (2H, s, H_4). ^{13}C NMR (75 MHz, CDCl_3): δ , ppm 142.1 (C_α), 141.3 (C-C_{meso}), 136.2 (CH_α), 135.0 (CH_α), 131.6 (CH_β), 128.9 (C-H_3), 127.9 (CH_p), 126.9 (CH_m), 126.8 (C-H_2), 126.6 (CH_m), 126.1 (C-H_4), 124.2 (C-H_1), 121.1. The C_{meso} , C-Cl, carbonyl and C-COO-Ru signals were not detected. UV-vis (CH_2Cl_2): λ_{max} , nm (log ϵ) 392 (5.42), 522 (4.24), 591 (4.25), 527 (sh). IR (ATR): ν , cm^{-1} 1735 ($\nu_{\text{C=O}}$), 1014 (oxidation marker band). Elemental analysis calcd. for $\text{C}_{102}\text{H}_{64}\text{Cl}_2\text{N}_8\text{O}_5\text{Ru}_2$ C, 69.82; H, 3.68; N, 6.39. Found C, 69.54; H, 3.42; N, 6.05. MS (ESI $^+$): m/z 1599 [$\text{M} - 155(m\text{CB})$] $^+$.

Synthesis of $\text{Ru}^{\text{II}}(\text{TPP})(4\text{-}^t\text{BuC}_6\text{H}_4\text{NH}_2)\text{CO}$ (17**).** The amine 4- $^t\text{BuC}_6\text{H}_4\text{NH}_2$ (97.6 μL , 6.13×10^{-4} mol) was added to a benzene (90 mL) suspension of $\text{Ru}(\text{TPP})\text{CO}$ (**15**) (150 mg, 2.02×10^{-4} mol). The resulting red solution was stirred at room temperature for 30 min, concentrated to 2 mL and *n*-hexane (20 mL) was added. The resulting red solid was collected by filtration and dried *in vacuo* (155 mg, 86%). ^1H NMR (300 MHz, C_6D_6): δ , ppm 8.83 (8H, s, H_β), 8.23 (4H, d, $J = 8.0$ Hz, H_α), 8.04 (4H, d, $J = 8.0$ Hz, H_α), 7.52 (8H, H_{m+p}), 7.40 (4H, H_m), 5.29 (2H, d, $J = 8.7$ Hz, H_{Ar}), 2.41 (2H, d, $J = 8.7$ Hz, H_{Ar}), 0.89 (9H, s, $\text{H}_{t\text{Bu}}$). ^{13}C NMR (75 MHz, C_6D_6): δ , ppm 144.6 (C), 143.0 (C), 135.1 (CH), 134.3 (CH), 132.5 (CH), 127.8 (CH), 126.6 (CH), 123.8 (CH). UV-vis (CH_2Cl_2): λ_{max} , nm (log ϵ) 413 (5.32), 532 (4.18). IR (ATR): ν , cm^{-1} 1948 ($\nu_{\text{C=O}}$), 1008 (oxidation marker band). Elemental analysis calcd. for $\text{C}_{55}\text{H}_{43}\text{N}_5\text{ORu}$ C, 74.14; H, 4.86; N, 7.86. Found C, 74.35; H, 4.95; N, 7.60. MS (ESI $^+$): m/z 892.6 [$\text{M} + 1$].

Synthesis of Ru^{VI}(TPP)(4'-BuC₆H₄N₃)₂ (18). The azide 4'-BuC₆H₄N₃ (32 mg, 1.8 × 10⁻⁴ mol) was added to a benzene (35 mL) solution of complex **3** (42.0 mg, 2.8 × 10⁻⁵ mol). The resulting dark mixture was refluxed for 8 h till the complete consumption of the organic azide (IR monitoring ν_{N=N} = 2124–2092 cm⁻¹). The solution was concentrated to 5 mL and *n*-hexane (15 mL) was added. By cooling the solution in an ice bath, the formation of a violet precipitate was observed. The dark violet solid was collected by filtration and dried *in vacuo*. (55% yield). ¹H NMR (300 MHz, C₆D₆): δ, ppm 8.93 (8H, s, H_β), 8.12 (8H, m, H_{Ph-ortho}), 7.47 (12H, m, H_{Ph-meta and -para}), 5.78 (4H, d, *J* = 8.7 Hz, H_{Ar-meta}), 2.77 (4H, d, *J* = 8.7 Hz, H_{Ar-ortho}), 0.64 (9H, s, H_{tBu}). ¹³C NMR (100 MHz, C₆D₆): δ, ppm 143.0 (C_o), 134.7 (CH_{Ph-ortho}), 131.6 (CH_β), 126.7 (CH_{Ph-meta and -para}), 123.1 (CH H_{Ar-meta}), 119.1 (CH_{Ar-ortho}), 30.75 (CH_{tBu}). A little amount of the complex decomposed during the carbon spectrum acquisition, five quaternary carbons were not detected. UV-vis (CH₂Cl₂): λ_{max}, nm (log ε) 39 (4.59), 532 (3.66). IR (ATR): ν, cm⁻¹ 2954 (ν_{C-H}), 1012 (oxidation marker band). Elemental analysis calcd. for C₆₄H₅₄N₆Ru C, 76.24; H, 5.40; N, 8.34. Found C, 76.55; H, 5.62; N, 8.11. MS (ESI⁺): *m/z* 1009.2 [M + 1].

Synthesis of [Ru^{IV}(TPP)(N₃)₂O (19). *Method A.* [Ru^{IV}(TPP)(OMe)₂O (**3**) (102 mg, 6.77 × 10⁻⁵ mol) was dissolved in benzene (20 mL) and trimethylsilyl azide was added (36 μl, 2.7 × 10⁻⁴ mol). The solution immediately turned from dark red to dark green, the mixture was stirred for 1 h at RT and monitored by TLC and IR analyses. The solution was evaporated to dryness and *n*-hexane (10 mL) was added to the residue. The resulting dark violet solid was collected by filtration and washed with *n*-hexane (10 mL) (90 mg, 87%). *Method B.* [Ru(TPP)(OMe)₂O (**3**) (108 mg, 7.17 × 10⁻⁵ mol) was dissolved in benzene (30 mL) and trityl azide was added (217 mg, 7.60 × 10⁻⁴ mol). The solution was heated to reflux for 4 h and the reaction was monitored by TLC and IR analyses. The solution was evaporated to dryness, the crude was washed with *n*-hexane (2 × 30 mL) and purified by chromatography (Al₂O₃, *n*-hexane/CH₂Cl₂ = 6:4). A dark violet solid was obtained (46 mg, 41%). ¹H NMR (300 MHz, CDCl₃): δ, ppm 8.87 (8H, d, *J* = 7.6 Hz, H_o), 8.65 (16H, s, H_β), 7.97 (8H, t, *J* = 7.6 Hz, H_m), 7.84 (8H, t, *J* = 7.5 Hz, H_p), 7.56 (8H, t, *J* = 7.5 Hz, H_m), 7.43 (8H, d, *J* = 7.6 Hz, H_o). ¹³C NMR (75 MHz, CDCl₃): δ, ppm 141.69 (C_o), 141.22 (C-C_{meso}), 136.27 (CH_o), 135.41 (CH_o), 131.78 (CH_β), 127.97 (CH_p), 127.00 (CH_m), 126.62 (CH_m), 120.83 (C_{meso}). UV-vis (CH₂Cl₂): λ_{max}, nm (log ε) 280 (4.43), 393 (5.46), 554 (4.18), 592 (4.21). IR (ATR): ν, cm⁻¹ 2023 (ν_{N=N}), 1012 (oxidation marker band). Elemental analysis calcd. for C₈₈H₅₆N₁₄ORu₂ C, 69.19; H, 3.69; N, 12.84; O, 1.05; Ru, 13.23. Found C, 69.31; H, 3.55; N, 12.47. MS (ESI⁺): *m/z* 1529.0 [M + 1]. X-ray quality crystals were obtained by slow diffusion of a CHCl₃ solution of [Ru(TPP)(N₃)₂O into *n*-hexane (see Table 2 and SI).

General procedure for catalytic reactions

Method A. In a typical run, complex **3** (39.0 mg, 2.60 × 10⁻⁵ mol) and the opportune amount of azide were dissolved into the desired hydrocarbon substrate (25 mL). The reaction solution was then heated to reflux by using a preheated oil bath. The consumption of the azide was monitored by TLC up to the point that its spot was no longer observable, and then by IR spectroscopy measuring the characteristic azide absorbance in the region 2095–2130 cm⁻¹. The reaction was considered to be finished when the absorbance of the latter peak was below 0.03 (using a 0.5 mm thick cell). The solution was then concentrated to dryness and the residue was purified by flash chromatography using *n*-hexane/ethyl acetate = 9:1 as the eluent mixture or analysed by ¹H NMR with 2,4-dinitrotoluene as the internal standard. All reaction times and products yields are reported in Table 1.

Method B. In a typical run, compound **3** (39.0 mg, 2.60 × 10⁻⁵ mol) and the opportune amount of azide and hydrocarbon were dissolved in benzene (25 mL). The solution was then heated to reflux by using a preheated oil bath. The consumption of the azide was monitored by TLC until its spot was no longer observable, and then by IR spectroscopy measuring the characteristic azide absorbance in the region 2095–2130 cm⁻¹. The reaction was considered to be finished when the absorbance of the latter peak was below 0.03 (using a 0.5 mm thick cell). The solution was then concentrated to dryness and the residue was purified by flash chromatography using *n*-hexane/ethyl acetate = 9:1 as the eluent mixture or analysed by ¹H NMR with 2,4-dinitrotoluene as the internal standard. All reaction times and products yields are reported in Table 1.

Single crystal X-ray diffraction of [Ru^{IV}(TPP)(N₃)₂O (19)

A crystal of species **19**, was mounted in air and used for X-ray structure determination. All measurements were made on a Rigaku Oxford Diffraction SuperNova area-detector diffractometer using mirror optics monochromated Mo Kα radiation (λ = 0.71073 Å) and Al filtered [35]. The unit cell constants and an orientation matrix for data collection were obtained from a least-squares refinement of the setting angles of reflections in the range 1.6° < θ < 25.2°. A total of 554 frames were collected using ω scans, with 15 + 15 s exposure time, a rotation angle of 1.0° per frame, a crystal-detector distance of 65.1 mm, at T = 173(2) K. Data reduction was performed using the CrysAlisPro program [36]. The intensities were corrected for Lorentz and polarization effects, and an absorption correction based on the multi-scan method using SCALE3 ABSPACK in CrysAlisPro was applied. Data collection and refinement parameters are given in Table 2.

The structure was solved by direct methods using SHELXS-97 [37], which revealed the positions of all

non-hydrogen atoms of the title compound. The non-hydrogen atoms were refined anisotropically. All H-atoms were placed in geometrically calculated positions and refined using a riding model where each H-atom was assigned a fixed isotropic displacement parameter with a value equal to 1.2Ueq of its parent atom.

Refinement of the structure was carried out on F^2 using full-matrix least-squares procedures, which minimised the function $\sum w(F_o^2 - F_c^2)^2$. The weighting scheme was based on counting statistics and included a factor to downweight the intense reflections. All calculations were performed using the SHELXL-97 program.

CONCLUSION

This work deals with the synthesis of μ -oxo dimeric ruthenium(IV) porphyrin species to investigate their catalytic efficiency in amination reactions by using aryl azides as nitrogen sources. Recorded data were compared to those achieved by using ruthenium(II) porphyrins in order to study the effect of the metal oxidation state on the catalytic performance of ruthenium porphyrin species. Similar catalytic results were achieved to indicate the probable formation of same active intermediates during the amination and in fact, the study of the reactivity of ruthenium(IV) species towards aryl azides disclosed the formation in both cases of a *bis*-imido ruthenium(VI) intermediate which is responsible for the nitrene transfer reaction. The stoichiometric reaction between $[\text{Ru}^{\text{IV}}(\text{TPP})(\text{OCH}_3)_2\text{O}]$ (**3**) and 4-*t*-BuC₆H₄N₃ or RN₃ (*R* = Ph₃C or (CH₃)₃Si) afforded $[\text{Ru}^{\text{VI}}(\text{TPP})(4\text{-}t\text{-BuC}_6\text{H}_4\text{N})_2]$ (**18**) and $[\text{Ru}^{\text{IV}}(\text{TPP})(\text{N}_3)_2\text{O}]$ (**19**) respectively. Both complexes were fully characterised and the molecular structure of complex **19** was determined by X-ray single crystal diffraction.

Supporting information

Table S1 is given in the supplementary material. This material is available free of charge *via* the Internet at <http://www.worldscinet.com/jpp/jpp.shtml>.

Crystallographic data have been deposited at the Cambridge Crystallographic Data Center (CCDC) under number CCDC-1450326. Copies can be obtained on request, free of charge, *via* www.ccdc.cam.ac.uk/data_request/cif or from the Cambridge Crystallographic Data Center, 12 Union Road, Cambridge CB2 1EZ, UK (fax: +44 1223-336-033 or email: data_request@ccdc.cam.ac.uk).

REFERENCES

1. Yamaguchi J, Yamaguchi AD and Itami K. *Angew Chem Int Ed* 2012; **51**: 8960–9009.
2. Uchida T and Katsuki T. *Chem. Rec.* 2014; **14**: 117–129.
3. Fantauzzi S, Caselli A and Gallo E. *Dalton Trans* 2009; 5434–5443.
4. Collet F, Lescot C and Dauban P. *Chem. Soc. Rev.* 2011; **40**: 1926–1936.
5. Chang JWW, Ton TMU and Chan PWH. *Chem. Rec.* 2011; **11**: 331–357.
6. Liu Y, Chen G-Q, Tse C-W, Guan X, Xu Z-J, Huang J-S and Che C-M. *Chem. Asian J.* 2015; **10**: 100–105.
7. Intriери D, Zardi P, Caselli A and Gallo E. *Chem. Commun.* 2014; **50**: 11440–11453.
8. Tseberlidis G, Zardi P, Caselli A, Cancogni D, Fusari M, Lay L and Gallo E. *Organometallics* 2015; **34**: 3774–3781.
9. Intriери D, Mariani M, Caselli A, Ragaini F and Gallo E. *Chem. Eur. J.* 2012; **18**: 10487–10490.
10. Intriери D, Caselli A, Ragaini F, Macchi P, Casati N and Gallo E. *Eur. J. Inorg. Chem.* 2012; 569–580.
11. Intriери D, Caselli A, Ragaini F, Cenini S and Gallo E. *J. Porphyrins Phthalocyanines* 2010; **14**: 732–740.
12. Manca G, Mealli C, Carminati DM, Intriери D and Gallo E. *Eur. J. Inorg. Chem.* 2015; 4885–4893.
13. Chan K-H, Guan X, Lo VK-Y and Che C-M. *Angew. Chem. Int. Ed.* 2014; **53**: 2982–2987.
14. Xiao W, Wei J, Zhou C-Y and Che C-M. *Chem. Commun.* 2013; **49**: 4619–4621.
15. Xiao W, Zhou C-Y and Che C-M. *Chem. Commun.* 2012; **48**: 5871–5873.
16. Guo Z, Guan X, Huang J-S, Tsui W-M, Lin Z and Che C-M. *Chem. Eur. J.* 2013; **19**: 11320–11331.
17. Fantauzzi S, Gallo E, Caselli A, Ragaini F, Casati N, Macchi P and Cenini S. *Chem. Commun.* 2009; 3952–3954.
18. Zardi P, Pozzoli A, Ferretti F, Manca G, Mealli C and Gallo E. *Dalton Trans.* 2015; **44**: 10479–10489.
19. Manca G, Gallo E, Intriери D and Mealli C. *ACS Catal.* 2014; 823–832.
20. Au S-M, Huang J-S, Yu W-Y, Fung W-H and Che C-M. *J. Am. Chem. Soc.* 1999; **121**: 9120–9132.
21. Collman JP, Barnes CE, Brothers PJ, Collins TJ, Ozawa T, Gallucci JC and Ibers JA. *J. Am. Chem. Soc.* 1984; **106**: 5151–5163.
22. Gallo E, Caselli A, Ragaini F, Fantauzzi S, Masciocchi N, Sironi A and Cenini S. *Inorg. Chem.* 2005; **44**: 2039–2049.
23. Groves JT and Quinn R. *Inorg. Chem.* 1984; **23**: 3844–3846.
24. Masuda H, Taga T, Osaki K, Sugimoto H, Mori M and Ogoshi H. *J. Am. Chem. Soc.* 1981; **103**: 2199–2203.
25. Vanover E, Huang Y, Xu L, Newcomb M and Zhang R. *Org. Lett.* 2010; **12**: 2246–2249.
26. Zhang R, Vanover E, Luo W and Newcomb M. *Dalton Trans.* 2014; **43**: 8749–8756.
27. Fantauzzi S, Gallo E, Caselli A, Piangiolino C, Ragaini F and Cenini S. *Eur. J. Org. Chem.* 2007; 6053–6059.
28. Collman JP, Boulatov R and Jameson GB. *Angew. Chem. Int. Ed.* 2001; **40**: 1271–1274.

29. Bortolini O, Campestrini S, Di Furia F and Modena G. *J. Org. Chem.* 1987; **52**: 5093–5095.
30. Tanno M, Sueyoshi S and Kamiya S. *Chem. Pharm. Bull.* 1982; **30**: 3125–3132.
31. Rillema DP, Nagle JK, Barringer LF Jr. and Meyer TJ. *J. Am. Chem. Soc.* 1981; **103**: 56–62.
32. Ragaini F, Penoni A, Gallo E, Tollari S, Li Gotti C, Lapadula M, Mangioni E and Cenini S. *Chem. Eur. J.* 2003; **9**: 249–259.
33. Zardi P, Caselli A, Macchi P, Ferretti F and Gallo E. *Organometallics* 2014; **33**: 2210–2218.
34. Caselli A, Gallo E, Fantauzzi S, Morlacchi S, Ragaini F and Cenini S. *Eur. J. Inorg. Chem.* 2008; 3009–3019.
35. Macchi P, Burgi H-B, Chimpri AS, Hauser J and Gal Z. *J. Appl. Crystallogr.* 2011; **44**: 763–771.
36. Rigaku-Oxford Diffraction. 2015 CrysAlisPro Version 171.37.33
37. Sheldrick G. *Acta Cryst. A* 2008; **64**: 112–122.